A Lentiviral Envelope Signal Sequence is a Tetherin Antagonizing Protein

James H. Morrison and Eric M. Poeschla*

Division of Infectious Diseases, University of Colorado Anschutz Medical Campus, Aurora, CO 80045, USA

Running Title: Fess Antagonizes Feline Tetherin

*Correspondence: Eric M. Poeschla, Mail Stop B168, Division of Infectious Diseases, University of Colorado Anschutz Medical Campus,12700 East 19th Avenue, Aurora, CO 80045. Tel: 303-724-8770. email: eric.poeschla@cuanschutz.edu

Key words: Tetherin, BST2, HIV-1, FIV, restriction factor, accessory protein, innate immunity, Signal Peptide, Signal Sequence, Leader Sequence

ABSTRACT

Signal sequences are N-terminal peptides, generally less than 30 amino acids in length, that direct translocation of proteins into the endoplasmic reticulum and secretory pathway. The envelope glycoprotein (Env) of the nonprimate lentivirus Feline immunodeficiency virus (FIV) contains the longest signal sequence of all eukaryotic, prokaryotic and viral proteins (175 amino acids). The reason is unknown. Tetherin is a dual membrane-anchored host protein that inhibits the release of enveloped viruses from cells. Primate lentiviruses have evolved three antagonists: the small accessory proteins Vpu and Nef, and in the case of HIV-2, Env. Here we identify the FIV Env signal sequence (Fess) as the FIV tetherin antagonist. A short deletion in the central portion of Fess had no effect on viral replication in the absence of tetherin but severely impaired virion budding in its presence. Fess is necessary and sufficient, acting as an autonomous accessory protein with the rest of Env dispensable. In contrast to primate lentivirus tetherin antagonists, it functions by stringently blocking the incorporation of this restriction factor into viral particles rather than by degrading it or downregulating it from the plasma membrane.

42 **INTRODUCTION**

43

44 The evolution of host antiviral factors has selected for reciprocal evolution of viral
45 countermeasures, which can act through passive avoidance or direct antagonism.
46 Tetherin (BST-2) is a type I interferon (IFN) inducible protein that forms homodimers and
47 directly links newly formed HIV-1 particles and the plasma membrane through its
48 transmembrane domain and a C-terminal GPI-anchor (Neil et al., 2008; Van Damme et
49 al., 2008). This attachment function prevents viral particle release from infected cells and
50 can lead to virus internalization, degradation via endosomal/lysosomal pathways, and
51 induction of NFκB-dependent pro-inflammatory responses in the infected cell (Cocka
52 and Bates, 2012; Galao et al., 2012; Miyakawa et al., 2009).

53 The importance of tetherin evasion for primate lentiviruses is indicated by their
54 nearly ubiquitous encoding of antagonists. Three different such proteins have been
55 described. SIVs of *Cercopithecus* genus primates (SIVgsn, SIVmus and SIVmon) and
56 HIV-1 counteract tetherin with the accessory protein Vpu (Sauter et al., 2009). SIVcpz,
57 the proximate precursor to HIV-1, shares common ancestry with cercopithecine SIVs yet
58 utilizes Nef to counteract tetherin (Sauter et al., 2009). Other SIVs also utilize Nef to
59 antagonize tetherin, including SIVsmm, the virus proximately ancestral to HIV-2 (Hirsch
60 et al., 1989; Jia et al., 2009; Zhang et al., 2009). A small deletion in the cytoplasmic tail
61 of human tetherin prevents Nef binding (Sauter et al., 2009). HIV-2 re-gained tetherin
62 antagonism in its envelope glycoprotein (Le Tortorec and Neil, 2009), whereas the HIV-1
63 subgroups, which arose from independent cross-species transmission events, vary in
64 this regard. Non-pandemic HIV-1 group O strains lack an efficient anti-tetherin
65 mechanism, but pandemic HIV-1 group M strains evolved a Vpu capable of
66 counteracting tetherin (Sauter et al., 2009). These primate lentiviral proteins all act by
67 functionally depleting tetherin from the plasma membrane via intracellular sequestration
68 or endocytosis and lysosomal degradation of the protein (Jia et al., 2009; Le Tortorec
69 and Neil, 2009; Zhang et al., 2009).

70 For non-primate lentiviruses, much less is known about viral interaction with and
71 evasion of tetherin. Their accessory gene repertoires are apparently more limited and
72 Vpu and Nef are found only in primate lentiviruses. For that matter, no new lentiviral
73 accessory genes have been identified for decades. Cat and dog tetherin proteins both
74 restrict HIV-1 and FIV and both carnivore proteins are antagonized by FIV Env (Morrison
75 et al., 2014). While this situation superficially resembles the antagonism of human

76 tetherin by HIV-2 Env, major differences were observed that suggest different
77 mechanisms. Unlike primate lentiviral antagonists, we found that the FIV Env
78 mechanism does not require processing of Env into its surface unit (SU) and
79 transmembrane (TM) domains (Morrison et al., 2014). It also shields the budding particle
80 without downregulating plasma membrane tetherin, and does not rescue non-cognate
81 (e.g., HIV-1) virus budding (Morrison et al., 2014). Here we explored the mechanism of
82 FIV tetherin antagonism further and determined that it derives specifically from the signal
83 sequence, which functions autonomously from Env, and acts to prevent particle
84 incorporation.
85

86 **RESULTS**

87

88 **Mapping of determinants of tetherin antagonism**

89 We previously reported that the envelope glycoprotein (Env) of FIV counteracts
90 restriction of this virus by both domestic cat and dog tetherin proteins and that this
91 activity is independent of proteolytic processing of Env into surface unit (SU) and
92 transmembrane (TM) domains (Morrison et al., 2014). FIV Rev and Env have the same
93 initiator methionine codon but are differentiated by alternative splicing; therefore, Rev
94 and Env of FIV share the first 80 amino acids (**Figure 1A**). To identify the minimal
95 components of Env necessary to enable nascent FIV virion escape from tetherin-
96 expressing cells, we constructed a series of Env frame-shift (efs) mutants that
97 progressively truncate the protein while leaving Rev intact. These were constructed in
98 FIVC36, an infectious molecular clone that replicates to high levels in vivo and causes
99 feline AIDS (de Rozieres et al., 2004). Antagonism of tetherin was determined by
100 quantifying FIV particles in cell supernatants following co-transfection of the FIV proviral
101 construct and tetherin plasmids (**Figure 1B**). Co-transfection of an Env-intact FIV with
102 increasing amounts of feline tetherin resulted in a modest reduction in reverse-
103 transcriptase (RT) activity and capsid (CA) in supernatants (**Figure 1B**, blue bars and
104 supernatant immunoblot). Introduction of a frameshift in the signal sequence of Env
105 (amino acid 90) resulted in a virus that was significantly more sensitive to the presence
106 of tetherin, with viral budding decreased in proportion to feline tetherin input (**Figure 1B**,
107 orange bars and immunoblot). In contrast, termination of Env in mid-SU, at residue 330,
108 reverted the phenotype, whereby again FIV was only modestly affected by tetherin co-
109 expression (**Figure 1B**, grey bars).

110 To further map the virus-rescuing activity in Env, a set of three additional
111 truncations was made by introducing frameshifts within the N-terminal portion of Env
112 (efs134, efs176 and efs248). These plus the initial efs90 and efs330 viruses were tested
113 for tetherin susceptibility, this time using cells that stably express either human or feline
114 tetherin (**Figure 2A**). As expected, each viral variant expressed equivalent intracellular
115 levels of FIV core proteins, budded in the absence of tetherin, and was blocked from
116 budding by human tetherin (**Figure 2A**). Absence of the Env SU or TM domains did not
117 significantly affect the ratio of intracellular Gag/CA to budded particles (efs176, efs248
118 and efs330). It was only when the signal sequence of Env was truncated (efs134 and
119 efs90) that a loss of FIV budding was observed in cells that express domestic cat

120 tetherin; again, human tetherin restriction was not abrogated) (**Figure 2A**). Quantification
121 of immunoblot densities confirmed that when normalized for intracellular capsid
122 expression levels feline tetherin was effective at blocking FIV budding of efs90 and
123 efs134, whereas wild-type FIVC36 and the efs mutants retaining at least the first 176
124 amino acids of Env were resistant to feline tetherin and even had higher ratios of
125 released to intracellular capsid compared to control cells lacking tetherin (**Figure 2B**).
126
127 **Fess is necessary and sufficient to counteract tetherin**
128 Considering these data, we hypothesized that the FIV Env signal sequence, which we
129 designate Fess, is the necessary factor that mediates feline tetherin antagonism. We
130 further hypothesized that it is sufficient (autonomously acting). Signal sequences, also
131 known as leader sequences or signal peptides, are N-terminal peptides that were
132 proposed in 1971 (Blobel and Sabatini, 1971) and subsequently established by Blöbel
133 and colleagues (Blobel and Dobberstein, 1975a, b) to act as cellular "zip codes" that
134 direct targeted translocation of newly synthesized proteins into the endoplasmic
135 reticulum (ER) lumen in a signal recognition particle-dependent manner. Analogous
136 subcellular targeting motifs, e.g., for mitochondria have also been described (Blobel,
137 2000). For enveloped viruses, signal sequences are the predominant mechanism
138 targeting viral surface proteins to the correct cellular compartment to enable proper
139 particle incorporation. In both eukaryotes and prokaryotes signal sequence lengths are
140 generally very short, with a mean length of 23 +/- 6 amino acids (Hiss and Schneider,
141 2009)). Primate lentiviruses encode somewhat longer Env signal sequences, ranging
142 between 19 and 45 amino acids in total length (**Figure S1**). Remarkably, our database
143 searches and literature reviews indicate that FIV encodes the longest known signal
144 sequence in any eukaryotic or prokaryotic species, or in any virus (175 amino acids).
145 Despite the identification of this unusual property over 25 years ago (Pancino et al.,
146 1993; Verschoor et al., 1993), the functional implications are unknown. To confirm that
147 the signal sequence is directly responsible for enabling viral budding in the presence of
148 domestic cat tetherin, and acts independently of other Env domains, we expressed it in
149 trans, as a fusion to an irrelevant but trackable protein, GFP (**Figure 3A**). We co-
150 expressed full-length Env, Fess-GFP, or a myc-epitope control protein (HIV Integrase)
151 with FIVC36 efs90 (**Figure 3B**). Viral budding was assessed by immunoblotting
152 supernatants with FIV antisera. As expected, FIVC36 efs90 budding was severely
153 impaired by either human or feline tetherin (**Figure 3B**, top). In contrast, co-expression

154 of either FIV Env or Fess-GFP rescued budding specifically in the presence of domestic
155 cat tetherin but not human tetherin (**Figure 3B**, middle and bottom). These results
156 highlight that Fess can function to counteract tetherin independently of other Env
157 domains and is sufficient for FIV antagonism of tetherin.
158
159 **Fess directs endoplasmic reticulum translocation and has dual function**
160 To further characterize the Fess protein for localization properties and to test if it can
161 fulfill traditional signal sequence functions in addition to acting as a tetherin antagonist,
162 we also examined the fate of Fess-GFP. In immunoblots for GFP, although Fess-GFP
163 was detectable, we observed intracellular accumulation of predominantly free GFP
164 (**Figure 3C**, left), indicating that Fess is efficiently cleaved from GFP at the signal
165 peptidase cleavage site. Free GFP was also detectable in the supernatant of Fess-GFP-
166 transfected but not GFP-transfected cells, indicating Fess directed GFP translocation
167 into the ER lumen and export via the secretory pathway (**Figure 3C**, right). Furthermore,
168 immunofluorescence experiments were strongly suggestive of localization in the ER for
169 the cleaved GFP signal in Fess-GFP expressing cells (**Figure 3D**). Confirming this, GFP
170 co-localized with the ER-resident protein calreticulin (**Figure 3E**) but not the Golgi
171 apparatus marker GORASP2 (**Figure 3F**). These experiments indicate that the majority
172 of the free GFP seen in Figure 2C is located in the ER. Cumulatively, the data confirm
173 that the FIV Env N-terminal 175 amino acids act as a bona fide signal sequence to direct
174 protein translocation.
175
176 **Deletion of a central Fess motif has no effect on viral replication in the absence of**
177 **tetherin but severely impairs virion release and viral replication in its presence**
178 Although signal sequences show no conservation of amino acid sequences, they are
179 functionally tripartite, with a positively charged N-terminal segment of variable length and
180 sequence, a single central hydrophobic core (H region), and a short C-terminal and
181 usually more conserved signal peptidase cleavage-site (Owji et al., 2018). In contrast to
182 this typical architecture, we identified two distinct hydrophobic segments in Fess, which
183 we designate H1 and H2 (**Figure 4A, B**). H1 is located in the central portion of Fess,
184 downstream of Rev exon 1 and upstream of the cleavage site-adjacent H2 motif. To test
185 the involvement of these regions in tetherin function, as well as viral viability and the
186 processing and trafficking of Env, we generated in-frame deletions in the full-length
187 virus. Mutant ΔH2/ΔC deletes the traditional signal sequence hydrophobic motif and

188 adjacent cleavage signal. Mutant Δ40 was designed to delete much of the region (40
189 amino acids) between the end of Rev first exon residues and the onset of the traditional
190 hydrophobic signal sequence and cleavage signal. The Δ40 deletion spans most of the
191 H1 hydrophobic motif (VFSILYLFTGYIVYFL) as well as a downstream region rich in
192 charged (R, K, D, E) residues (**Figure 4A**). FIV C36Δ40 retained Env expression and
193 normal replication kinetics in feline CrFK cells, whereas the FIV C36ΔH2/ΔC mutant had
194 much lower Env protein expression in cells and greatly diminished replication (**Figure**
195 **4C, D**). Wild type FIV was inhibited by human but not feline tetherin as expected (**Figure**
196 **4E**). In contrast, the Δ40 mutation had two notable effects. It resulted in increased
197 budding compared to wild type virus (compare black bars) in the absence of feline
198 tetherin, but resulted in severe restriction in its presence (**Figure 4E**). Feline but not
199 human tetherin restriction was selectively abrogated if these 40 amino acids were intact.
200 These results, combined with the above observations, confirm that Fess confers
201 resistance to domestic cat tetherin restriction of viral release from cells. Furthermore, the
202 effects of Fess on Env SU/TM expression and trafficking to the cell surface are
203 separable from its tetherin antagonism function.
204
205 **Fess acts by blocking tetherin Incorporation into particles**
206 Our previous data suggested that FIV antagonizes tetherin by a mechanism more similar
207 to that of Ebola virus than that mediated by primate lentivirus accessory genes (Morrison
208 et al., 2014). Both viruses act in a way that is linked to their respective Env glycoproteins
209 but does not reduce cell surface or intracellular tetherin levels (Kuhl et al., 2011; Lopez
210 et al., 2010; Morrison et al., 2014); see also **Figure 2A** here. This observation suggested
211 to us a mechanism that acts locally, on a per-particle basis at the point of viral budding,
212 to exclude the factor from the particle (Morrison et al., 2014). To determine whether Fess
213 alters the particle association of tetherin, wild type or Δ40 FIV particles were produced in
214 the presence or absence of stably expressed tetherins and then purified by
215 ultracentrifugation over a sucrose cushion. Particles were then immunoblotted – using
216 reverse transcriptase-normalized inputs – for tetherin. The results were dramatic. Wild-
217 type FIVC36 virions contained minimal amounts of human or feline tetherin (**Figure 5**).
218 In contrast, FIVC36Δ40 virions contained similarly low levels of human tetherin, but high
219 levels of feline tetherin (**Figure 5**). Thus, the activity of Fess is both powerful and
220 specific: intact Fess stringently blocks otherwise abundant virion incorporation of feline

221 but not human tetherin. This mechanism is also unique among the lentiviral anti-
222 tetherins.
223
224

225 **DISCUSSION**

226

227 Our results reveal that the Env glycoprotein signal sequence is the FIV tetherin
228 antagonist, thus identifying the fourth lentiviral anti-tetherin protein and also, to the best
229 of our knowledge, identifying the first new lentiviral accessory protein in decades. Almost
230 all of Env – all of the SU and TM domains – was entirely dispensable for tetherin
231 antagonism. Fess was both necessary and sufficient for enabling release of viral
232 particles from tetherin expressing cells (**Figure 1-4**). We identified a central 40 amino
233 acid segment of Fess that is located C-terminal to the first exon of Rev, is not needed for
234 Env processing, and the function of which was previously unknown. Deletion of the
235 segment did not affect FIV replication in the absence of tetherin but severely impaired
236 budding of the virus in its presence. The mechanism fulfills multiple criteria for a
237 specifically evolved restriction factor antagonism, as it is also virus- and species-specific:
238 Fess did not protect FIV from human tetherin, or HIV-1 from either feline or human
239 tetherin (**Figures 2 & 4E** and (Morrison et al., 2014)).

240 Simple retroviruses encode *gag*, *pol* and *env* genes that primarily encode the
241 structural and enzymatic proteins needed for completing essential viral lifecycle steps.
242 Lentiviruses, by contrast, are complex retroviruses that establish persistent, lifelong
243 infections and must therefore evade innate and adaptive immunity for years. To meet
244 this challenge, they have evolved additional accessory proteins that modulate host
245 immune responses and antagonize innate immune effectors. HIV-1 and simian
246 lentiviruses variably use the small accessory proteins Vpu and Nef to overcome the
247 block to nascent viral budding imposed by tetherin, which appears to have afforded
248 genetic flexibility. The evolution of these proteins not only underlies persistence in a
249 given species, but has also been shown to be critical for host switching, as in the case of
250 the acquisition of Vpu during the adaptation of SIVcpz to become HIV-1 (Neil, 2017;
251 Sauter et al., 2009). Presumably due to the pressures posed by such viral proteins and
252 also from non-retroviral antagonists, tetherin proteins show evidence of positive
253 selection in mammals (Lim et al., 2010; Liu et al., 2010; McNatt et al., 2009).

254 Non-primate lentiviruses encode more limited accessory gene repertoires than
255 primate lentiviruses and they specifically lack Vpu and Nef proteins. The prior mapping
256 of anti-tetherin activity to the *Env* gene of FIV suggested antagonism by the full Env
257 glycoprotein similar to what has been observed for HIV-2 (Celestino et al., 2012; Dietrich
258 et al., 2011; Le Tortorec and Neil, 2009; Morrison et al., 2014). However, our data reveal

259 that FIV SU and TM are dispensable. We showed previously that FIV does not degrade
260 tetherin or down-regulate it from the cell surface (Morrison et al., 2014), identifying a
261 contrast with primate lentiviral Vpu, Nef or Env proteins, which all mediate functional
262 depletion of tetherin from the primary site of viral budding via intracellular sequestration,
263 endocytosis and lysosomal degradation of the protein (Jia et al., 2009; Le Tortorec and
264 Neil, 2009; Zhang et al., 2009). Here we show that Fess instead excludes tetherin from
265 the particle, establishing a mechanism unique among the lentiviruses (**Figure 5**). Fess
266 possesses autonomous restriction blocking activity and can also direct the ER
267 translocation and export of an unrelated protein (**Figure 3**).
268 Signal sequences (signal peptides) act as intracellular zip codes that direct the
269 location of many cellular proteins that are destined for extra-cytoplasmic locations.
270 Proteins destined for secretion or plasma membrane residence are translocated as
271 preproteins through or into the ER membrane. After preprotein translocation has partially
272 completed, the signal peptidase enzyme cleaves the signal sequence away, which
273 enables correct folding of the mature protein. Signal sequences are generally quite short
274 (under 30 amino acids), do not have further functions, and are mostly degraded in short
275 order by the signal peptide peptidase. In the case of RNA viruses, however, genome
276 sizes are severely constrained and, for retroviruses, genetic efficiency in the form of
277 overlapping reading frames and multiple purpose proteins, e.g., Nef, are observed. Dual
278 purposing of the signal sequence by FIV is an interesting example. The amino acids
279 encoded by the first exon of Rev are also present in the first 80 amino acids of Fess,
280 which adds a third function to this compressed region of the genome. There are a few
281 prior examples of cellular protein signal sequences with additional cellular functions
282 (Martoglio and Dobberstein, 1998) and a few in other viruses as well. However, the latter
283 generally involve direct participation in mechanics of the virus's replication machinery.
284 Following signal peptidase processing of the Arenavirus envelope glycoprotein, the
285 signal sequence is not degraded and instead forms a tripartite complex with the mature
286 glycoprotein subunits, which is necessary for glycoprotein mediated fusion with target
287 cells (Nunberg and York, 2012). In this case the signal sequence function remains tied to
288 that of the envelope protein. Among retroviruses, the spumaretrovirus foamy virus signal
289 sequence binds to cognate Gag molecules and is packaged into viral particles, where it
290 appears to be necessary for proper virion morphogenesis (Geiselhart et al., 2003;
291 Lindemann et al., 2001). The signal sequences of the betaretroviruses mouse mammary
292 tumor virus (Dultz et al., 2008) and Jaagsiekte sheep retrovirus (Caporale et al., 2009)

293 Env proteins traffic to the nucleoli of infected cells, where they are involved in modulating
294 nuclear export of unspliced viral mRNAs.
295 In the case of Fess, the signal sequence has evolved to counter a main host
296 defense and can properly be considered a viral accessory protein. We propose that Env
297 signal sequences with additional functions independent of directing Env translocation
298 may in fact be a more general non-primate lentivirus property, since the signal
299 sequences of these viruses vary in length but are all significantly longer (66-176 amino
300 acids, **Figure S1**) than the signal sequences of primate lentiviruses and most cellular
301 signal sequences (Martoglio and Dobberstein, 1998; Pancino et al., 1994). Indeed, the
302 full length equine infectious anemia virus Env glycoprotein has been reported to
303 counteract horse tetherin, also by a mechanism that does not degrade the factor;
304 whether all or just part of Env is the antagonist has not been determined (Yin et al.,
305 2014).
306 Our results underscore the centrality of tetherin to mammalian defense against
307 lentiviruses in widely different circumstances. Feline and primate lentiviruses share
308 distant ancestry, with the former likely to have colonized some but not all feline lineages
309 sometime after the modern felid species radiation in the late Miocene, c.a. 11 million
310 years ago (Mya) (Pecon-Slattery et al., 2008). Major commonalities do persist between
311 FIV and HIV in pathophysiology (AIDS) and dependency factor utilization, such as
312 CXCR4 and LEDGF, and both have Vif proteins that degrade APOBEC3 proteins (Llano
313 et al., 2006; Münk et al., 2008; Poeschla and Looney, 1998). Domestic cat FIV is an
314 AIDS-causing lentivirus like HIV-1, yet it and its ancestral felid species relatives have
315 been on an independent evolutionary trajectory for millions of years. On the host side of
316 the equation, the tiger and the domestic cat tetherin proteins share a likely more ancient
317 (c.a. 60 to 11 Mya) truncation of the cytoplasmic tail, with the loss of 19 of 27 amino
318 acids, including a dual tyrosine motif (Morrison et al., 2014). The parallel evolution by
319 FIV of an anti-tetherin protein that is structurally, functionally and mechanistically very
320 different from those of the primate lentivirus proteins in consistent with this and other
321 evidence for the genetic plasticity of this host factor. The unusual architecture of
322 tetherins rather than primary sequence is critical for their function, as well as their
323 versatility against other groups of enveloped viruses (Blanco-Melo et al., 2016;
324 Heusinger et al., 2015; Perez-Caballero et al., 2009). Investigation of other lentiviruses
325 may uncover further viral solutions to the problem of tetherin.

326 **MATERIALS AND METHODS**

327

328 **Cells.** 239T and Crandell feline kidney (CrFK) cells were cultured in DMEM with 10%
329 fetal calf serum (FBS), penicillin-streptomycin, and L-glutamine. Stable HA-tetherin
330 expressing cells have been previously described (Morrison et al., 2014) and were
331 additionally cultured in 3 µg/mL puromycin.

332

333 **Vectors, viruses and plasmids.** pCT-C36^{A+} and pFE-C36 (subclone encoding Env
334 protein) were used as the basis for mutagenesis (Morrison et al., 2014). They employ
335 the 5 'U3-replacement strategy that enabled FIV production in human cells, in which the
336 FIV U3 has virtually no promoter function) (Poeschla and Looney, 1998; Poeschla et al.,
337 1998). In this case we applied this to the proviral clone C36 (de Rozieres et al., 2004),
338 Additionally C36 *Env* was subcloned from NheI-digested pCT-C36^{A+} into the NheI site of
339 gammaretroviral vector pJZ308 (Poeschla and Looney, 1998) to yield pJZC36. Env-
340 frameshift mutants of C36 were constructed within pFE-C36 by site directed
341 mutagenesis (Efs330) or overlap-extension PCR between NotI and MfeI restriction
342 enzyme sites, approximately comprising *Env* amino acids 1-500. Insertions to frameshift
343 Env are denoted here (lower-case letter indicates inserted nucleotide, enzyme in
344 parentheses indicates restriction site added by nucleotide insertion):
345 Efs90: GGTAAGATATTTAAGATAtCTCTGATTTACAAGTATTTAG (EcoRV)
346 Efs134: CTGGGGAAAAATTTAatTAAAAATGAAAAGGGAC (PacI)
347 Efs176: GACAAGGTAAGGCACAAGctTAATATGGAGACTCCCACCC (HindIII)
348 Efs247: GAAAGCTACAAGAtAATcTAGAAGGGGAAAAGTTTGG (XbaI)
349 Efs330: CAAATCCCACTGATCAATTAgtcgacagTACATTTGGACCTAATC (ScaI)
350 Mutants were verified by restriction enzyme digestion and sequencing across the cloned
351 fragment. An AvrII/BglII fragment from pFE-C36 was then moved into pJZ C36
352 (AvrII/BglII), then an NheI fragment from pJZ C36 was then swapped into an NheI
353 digested pCT-C36 to create pCT-C36 mutants with the indicated insertions causing *Env*
354 frame-shift but no other changes. Each mutant was again verified by sequencing across
355 the entire NheI fragment. C36Δ40 and C36ΔH2/ΔC were cloned by overlap extension
356 PCR to remove 40 amino acids (residues 99-138) or 29 amino acids (ΔH2/ΔC, residues
357 150-178), and re-inserted between AvrII and EcoNI digested pJZ C36, then an NheI
358 fragment of pJZC36Δ40 or ΔH2 containing C36 *Env* was again inserted back into NheI
359 digested pCT-C36^{A+}. Codon optimized Fess (amino acids 1-178) was synthesized as a

360 gBlock (IDT). Complementary Fess and GFP cDNAs were generated by PCR and
361 cloned into a NotI/BglII digested p1012 IN-myc (Vanegas et al., 2005) using the GeneArt
362 Seamless Cloning System (ThermoFisher), with a single amino acid linker (S) separating
363 Fess and GFP.
364
365 **Transfections and particle analyses.** $4x10^5$ 293T cells were plated per well of a 6-well
366 plate, allowed to adhere overnight, and PEI transfected. 1.5 g total DNA was added to
367 35 µL of Optimem without serum and 6 µL of 1 µg/µL PEI before brief vortexing and
368 incubation at room temperature for 30min. Transfection mix was added drop-wise to
369 cells and washed with fresh complete media after 8-16 hours. 48 hours post-
370 transfection, supernatant was harvested and filtered through a 0.45 µM filter. For
371 analysis of tetherin incorporation into viral particles, supernatant was concentrated by
372 ultracentrifugation over a 20% sucrose cushion. At the time of supernatant harvest, cells
373 were lysed in 1x radioimmunoprecipitation (RIPA) buffer (150 mM NaCl, 0.5%
374 deoxycholate, 0.1% sodium dodecyl sulfate, 1% NP-40, 150 mM Tris-HCl pH8.0).
375 Immunoblotting was performed with cat serum reactive to FIV-PPR (gift of Peggy Barr),
376 rat α-HA (Roche), mouse anti-GFP (JL-8 clone, Takara Bio) or mouse anti-alpha-tubulin
377 (Sigma). Immunoblot band density was quantified using ImageJ.
378
379 **Reverse-transcriptase activity.** Reverse-transcriptase (RT) activity was quantified by
380 use of a real-time PCR assay as previously described (Vermeire et al., 2012). 5 µL of
381 supernatant was mixed with 5 µL of 2x viral lysis buffer (0.25% Triton X-100, 50 mM
382 KCL, 100 mM TrisHCL, pH 7.4, 40% glycerol, and 2% v/v RNAse inhibitor) and
383 incubated at room temperature for 10 minutes, then 90 µL of sterile water was added.
384 Samples were diluted 1:100 in sterile water, then 9 µL of diluted, lysed sample was used
385 in a 20 µL qPCR reaction containing 10 µL of 2x SYBR Green master mix (Apex Sybr
386 Green, Quintarabio), 120 nM MS2 cDNA primers, and 0.055 A_{260} units of MS2 RNA
387 (Sigma, catalog # 10165948001).
388
389 **Immunofluorescence.** 1 x 10^5 293T cells were plated on LabTek II chamber slides,
390 allowed to adhere overnight and transfected with 500 ng indicated plasmids (pEGFP-N1
391 or pFess-GFP). 48 hours post-transfection cells were fixed with 4% (wt/vol)
392 paraformaldehyde for 10 minutes at room temperature, permeabilized with methanol,
393 stained for 1 hour at room temperature with rabbit anti-Calreticulin (1:50, Abcam

394 ab2907) or anti-GORASP2 (1:100, Sigma HPA035274), washed 3x with PBS and
395 stained for 1 hour at room temperature with Alexafluor 594-anti-rabbit-IgG (1:500). Wells
396 were again washed 3x with PBS then mounted with ProLong Gold antifade reagent with
397 DAPI (Invitrogen P36935). Images were collected on a Zeiss LSM780.
398
399
400
401 **ACKNOWLEDGMENTS**
402
403 Supported by NIH grant AI77344 and DP1DA043915. Imaging experiments used the
404 Advanced Light Microscopy Core at the Anschutz Medical Campus, which is supported
405 by NIH NS048154 and DK116073. We thank other laboratory members for helpful
406 suggestions.
407
408
409 **AUTHOR CONTRIBUTIONS**
410
411 J.H.M and E.M.P formulated ideas, hypotheses, and experimental approaches.
412 J.H.M performed experiments. J.H.M and E.M.P analyzed and interpreted data
413 and wrote the manuscript.

414 **REFERENCES**
415

416 Blanco-Melo, D., Venkatesh, S., and Bieniasz, P.D. (2016). Origins and Evolution of tetherin, an Orphan
417 Antiviral Gene. Cell host & microbe *20*, 189-201.
418 Blobel, G. (2000). Protein targeting (Nobel lecture). Chembiochem *1*, 86-102.
419 Blobel, G., and Dobberstein, B. (1975a). Transfer of proteins across membranes. I. Presence of proteolytically
420 processed and unprocessed nascent immunoglobulin light chains on membrane-bound ribosomes of
421 murine myeloma. The Journal of cell biology *67*, 835-851.
422 Blobel, G., and Dobberstein, B. (1975b). Transfer of proteins across membranes. II. Reconstitution of
423 functional rough microsomes from heterologous components. The Journal of cell biology *67*, 852-862.
424 Blobel, G., and Sabatini, D. (1971). Ribosome-membrane interaction in eukaryotic cells. In Biomembranes, L.
425 Manson, ed. (Plenum Publishing Corporation), pp. 193-195.
426 Caporale, M., Arnaud, F., Mura, M., Golder, M., Murgia, C., and Palmarini, M. (2009). The signal peptide of a
427 simple retrovirus envelope functions as a posttranscriptional regulator of viral gene expression. Journal
428 of virology *83*, 4591-4604.
429 Celestino, M., Calistri, A., Del Vecchio, C., Salata, C., Chiuppesi, F., Pistello, M., Borsetti, A., Palu, G., and
430 Parolin, C. (2012). Feline tetherin is characterized by a short N-terminal region and is counteracted by
431 the feline immunodeficiency virus envelope glycoprotein. Journal of virology *86*, 6688-6700.
432 Cocka, L.J., and Bates, P. (2012). Identification of alternatively translated Tetherin isoforms with differing
433 antiviral and signaling activities. PLoS pathogens *8*, e1002931.
434 de Rozieres, S., Mathiason, C.K., Rolston, M.R., Chatterji, U., Hoover, E.A., and Elder, J.H. (2004).
435 Characterization of a highly pathogenic molecular clone of feline immunodeficiency virus clade C. Journal
436 of virology *78*, 8971-8982.
437 Dietrich, I., McMonagle, E.L., Petit, S.J., Vijayakrishnan, S., Logan, N., Chan, C.N., Towers, G.J., Hosie, M.J.,
438 and Willett, B.J. (2011). Feline tetherin efficiently restricts release of feline immunodeficiency virus but not
439 spreading of infection. Journal of virology *85*, 5840-5852.
440 Dultz, E., Hildenbeutel, M., Martoglio, B., Hochman, J., Dobberstein, B., and Kapp, K. (2008). The signal
441 peptide of the mouse mammary tumor virus Rem protein is released from the endoplasmic reticulum
442 membrane and accumulates in nucleoli. The Journal of biological chemistry *283*, 9966-9976.
443 Galao, R.P., Le Tortorec, A., Pickering, S., Kueck, T., and Neil, S.J. (2012). Innate sensing of HIV-1 assembly
444 by Tetherin induces NFkappaB-dependent proinflammatory responses. Cell host & microbe *12*, 633-644.
445 Geiselhart, V., Schwantes, A., Bastone, P., Frech, M., and Lochelt, M. (2003). Features of the Env leader
446 protein and the N-terminal Gag domain of feline foamy virus important for virus morphogenesis. Virology
447 *310*, 235-244.
448 Heusinger, E., Kluge, S.F., Kirchhoff, F., and Sauter, D. (2015). Early Vertebrate Evolution of the Host
449 Restriction Factor Tetherin. Journal of virology *89*, 12154-12165.
450 Hirsch, V.M., Olmsted, R.A., Murphey-Corb, M., Purcell, R.H., and Johnson, P.R. (1989). An African primate
451 lentivirus (SIVsm) closely related to HIV-2. Nature *339*, 389-392.
452 Hiss, J.A., and Schneider, G. (2009). Domain organization of long autotransporter signal sequences. Bioinform
453 Biol Insights *3*, 189-204.
454 Jia, B., Serra-Moreno, R., Neidermyer, W., Rahmberg, A., Mackey, J., Fofana, I.B., Johnson, W.E.,
455 Westmoreland, S., and Evans, D.T. (2009). Species-specific activity of SIV Nef and HIV-1 Vpu in
456 overcoming restriction by tetherin/BST2. PLoS pathogens *5*, e1000429.
457 Kuhl, A., Banning, C., Marzi, A., Votteler, J., Steffen, I., Bertram, S., Glowacka, I., Konrad, A., Sturzl, M., Guo,
458 J.T.*, et al.* (2011). The Ebola virus glycoprotein and HIV-1 Vpu employ different strategies to counteract
459 the antiviral factor tetherin. J Infect Dis *204 Suppl 3*, S850-860.
460 Le Tortorec, A., and Neil, S.J. (2009). Antagonism to and intracellular sequestration of human tetherin by the
461 human immunodeficiency virus type 2 envelope glycoprotein. Journal of virology *83*, 11966-11978.
462 Lim, E.S., Malik, H.S., and Emerman, M. (2010). Ancient adaptive evolution of tetherin shaped the functions
463 of Vpu and Nef in human immunodeficiency virus and primate lentiviruses. J Virol *84*, 7124-7134.
464 Lindemann, D., Pietschmann, T., Picard-Maureau, M., Berg, A., Heinkelein, M., Thurow, J., Knaus, P.,
465 Zentgraf, H., and Rethwilm, A. (2001). A particle-associated glycoprotein signal peptide essential for virus
466 maturation and infectivity. Journal of virology *75*, 5762-5771.
467 Liu, J., Chen, K., Wang, J.H., and Zhang, C. (2010). Molecular evolution of the primate antiviral restriction
468 factor tetherin. PloS one *5*, e11904.
469 Llano, M., Saenz, D.T., Meehan, A., Wongthida, P., Peretz, M., Walker, W.H., Teo, W., and Poeschla, E.M.
470 (2006). An Essential Role for LEDGF/p75 in HIV Integration. Science *314*, 461-464.
471 Lopez, L.A., Yang, S.J., Hauser, H., Exline, C.M., Haworth, K.G., Oldenburg, J., and Cannon, P.M. (2010).
472 Ebola virus glycoprotein counteracts BST-2/Tetherin restriction in a sequence-independent manner that
473 does not require tetherin surface removal. Journal of virology *84*, 7243-7255.

474 Martoglio, B., and Dobberstein, B. (1998). Signal sequences: more than just greasy peptides. Trends Cell Biol
475 *8*, 410-415.
476 McNatt, M.W., Zang, T., Hatziioannou, T., Bartlett, M., Fofana, I.B., Johnson, W.E., Neil, S.J., and Bieniasz,
477 P.D. (2009). Species-specific activity of HIV-1 Vpu and positive selection of tetherin transmembrane
478 domain variants. PLoS Pathog *5*, e1000300.
479 Miyakawa, K., Ryo, A., Murakami, T., Ohba, K., Yamaoka, S., Fukuda, M., Guatelli, J., and Yamamoto, N.
480 (2009). BCA2/Rabring7 promotes tetherin-dependent HIV-1 restriction. PLoS pathogens *5*, e1000700.
481 Morrison, J.H., Guevara, R.B., Marcano, A.C., Saenz, D.T., Fadel, H.J., Rogstad, D.K., and Poeschla, E.M.
482 (2014). Feline immunodeficiency virus envelope glycoproteins antagonize tetherin through a distinctive
483 mechanism that requires virion incorporation. Journal of virology *88*, 3255-3272.
484 Münk, C., Beck, T., Zielonka, J., Hotz-Wagenblatt, A., Chareza, S., Battenberg, M., Thielebein, J., Cichutek,
485 K., Bravo, I.G., O'Brien, S.J*., et al.* (2008). Functions, structure, and read-through alternative splicing of
486 feline APOBEC3 genes. Genome Biol *9*, R48.
487 Neil, S.J. (2017). Exercising Restraint. Cell Host Microbe *21*, 274-277.
488 Neil, S.J., Zang, T., and Bieniasz, P.D. (2008). Tetherin inhibits retrovirus release and is antagonized by HIV-
489 1 Vpu. Nature *451*, 425-430.
490 Nunberg, J.H., and York, J. (2012). The curious case of arenavirus entry, and its inhibition. Viruses *4*, 83-101.
491 Owji, H., Nezafat, N., Negahdaripour, M., Hajiebrahimi, A., and Ghasemi, Y. (2018). A comprehensive review
492 of signal peptides: Structure, roles, and applications. Eur J Cell Biol *97*, 422-441.
493 Pancino, G., Ellerbrok, H., Sitbon, M., and Sonigo, P. (1994). Conserved framework of envelope glycoproteins
494 among lentiviruses. Curr Top Microbiol Immunol *188*, 77-105.
495 Pancino, G., Fossati, I., Chappey, C., Castelot, S., Hurtrel, B., Moraillon, A., Klatzmann, D., and Sonigo, P.
496 (1993). Structure and variations of feline immunodeficiency virus envelope glycoproteins. Virology *192*,
497 659-662.
498 Pecon-Slattery, J., Troyer, J.L., Johnson, W.E., and O'Brien, S.J. (2008). Evolution of feline immunodeficiency
499 virus in Felidae: implications for human health and wildlife ecology. Veterinary immunology and
500 immunopathology *123*, 32-44.
501 Perez-Caballero, D., Zang, T., Ebrahimi, A., McNatt, M.W., Gregory, D.A., Johnson, M.C., and Bieniasz, P.D.
502 (2009). Tetherin inhibits HIV-1 release by directly tethering virions to cells. Cell *139*, 499-511.
503 Poeschla, E., and Looney, D. (1998). CXCR4 is required by a non-primate lentivirus: heterologous expression
504 of feline immunodeficiency virus in human, rodent and feline cells. Journal of virology *72*, 6858-6866.
505 Poeschla, E., Wong-Staal, F., and Looney, D. (1998). Efficient transduction of nondividing cells by feline
506 immunodeficiency virus lentiviral vectors. Nature medicine *4*, 354-357.
507 Sauter, D., Schindler, M., Specht, A., Landford, W.N., Munch, J., Kim, K.A., Votteler, J., Schubert, U., Bibollet-
508 Ruche, F., Keele, B.F*., et al.* (2009). Tetherin-driven adaptation of Vpu and Nef function and the evolution
509 of pandemic and nonpandemic HIV-1 strains. Cell host & microbe *6*, 409-421.
510 UniProt Consortium, T. (2018). UniProt: the universal protein knowledgebase. Nucleic acids research *46*,
511 2699.
512 Van Damme, N., Goff, D., Katsura, C., Jorgenson, R.L., Mitchell, R., Johnson, M.C., Stephens, E.B., and
513 Guatelli, J. (2008). The interferon-induced protein BST-2 restricts HIV-1 release and is downregulated
514 from the cell surface by the viral Vpu protein. Cell host & microbe *3*, 245-252.
515 Vanegas, M., Llano, M., Delgado, S., Thompson, D., Peretz, M., and Poeschla, E. (2005). Identification of the
516 LEDGF/p75 HIV-1 integrase-interaction domain and NLS reveals NLS-independent chromatin tethering.
517 J Cell Sci *118*, 1733-1743.
518 Vermeire, J., Naessens, E., Vanderstraeten, H., Landi, A., Iannucci, V., Van Nuffel, A., Taghon, T., Pizzato,
519 M., and Verhasselt, B. (2012). Quantification of reverse transcriptase activity by real-time PCR as a fast
520 and accurate method for titration of HIV, lenti- and retroviral vectors. PloS one *7*, e50859.
521 Verschoor, E.J., Hulskotte, E.G., Ederveen, J., Koolen, M.J., Horzinek, M.C., and Rottier, P.J. (1993). Post-
522 translational processing of the feline immunodeficiency virus envelope precursor protein. Virology *193*,
523 433-438.
524 Yin, X., Hu, Z., Gu, Q., Wu, X., Zheng, Y.H., Wei, P., and Wang, X. (2014). Equine tetherin blocks retrovirus
525 release and its activity is antagonized by equine infectious anemia virus envelope protein. J Virol *88*,
526 1259-1270.
527 Zhang, F., Wilson, S.J., Landford, W.C., Virgen, B., Gregory, D., Johnson, M.C., Munch, J., Kirchhoff, F.,
528 Bieniasz, P.D., and Hatziioannou, T. (2009). Nef proteins from simian immunodeficiency viruses are
529 tetherin antagonists. Cell host & microbe *6*, 54-67.
530
531

532 **FIGURE LEGENDS**

533

534 **Figure 1. SU and TM are dispensable for tetherin antagonism. (A)** Diagram of FIV
535 *Env* gene. Numbering indicates amino acids from the Env initiator methionine, which is
536 shared with Rev. **(B)** 293T cells were co-transfected with pFIVC36 proviral constructs
537 (pCT-C36^{A+} based) encoding an intact Env (blue bars), or an Env frame-shift (efs)
538 mutation at amino acid 90 (orange bars) or at amino acid 330 (grey bars). Diagrams
539 indicate Env subunits intact (green) or disrupted (grey). Cell lysates and supernatant
540 were harvested 48 hours after transfection and immunoblotted with the indicated primary
541 antibody and a corresponding HRP-conjugated secondary antibody. Experiment was
542 repeated four times and a representative example is shown.

543

544 **Figure 2. Effects of N-terminal deletions on feline tetherin restriction. (A)** 293T cells
545 having the indicated tetherin stably expressed under puromycin selection were
546 transfected with the indicated pC36 proviral construct. Numbering indicates the last
547 intact Env amino acid before early protein termination due to a frameshifting mutation.
548 48 hours after transfection cell lysates and supernatants were harvested and analyzed
549 as in panel A. **(B)** Bands corresponding to FIV capsid from panel A were density
550 quantified using ImageJ. The ratio of the supernatant to intracellular capsid band were
551 calculated and normalized to FIVC36 from cells without tetherin. Lane numbers are the
552 same as panel A. Experiment was repeated four times and a representative example is
553 shown.

554

555 **Figure 3. Fess is sufficient to counteract domestic cat tetherin and can direct**
556 **protein translocation into the secretory pathway. (A)** Diagram of the Fess-GFP
557 construct. **(B)** 293T cells stably expressing tetherin were transfected as in Figure 1 with
558 1 µg pC36 EFS90 and 0.5 µg p1012-myc (control), p1012 SS-GFP, or pFE-C36 (full-
559 length C36 Envelope). Equal volume supernatant was harvested 48 hours post-
560 transfection, immunoblotted with cat sera reactive to FIV and viral capsid bands are
561 shown. Experiment was repeated three times and a representative example is shown.
562 **(C)** 293T cells were transfected with plasmids that express eGFP, myc-tagged HIV-1
563 integrase (negative control for blot), or Fess-GFP (pEGFP-N1, p1012 -HIV-1-IN-myc,
564 pFess-GFP) and cell lysates and supernatants were collected 48 hours post-transfection
565 and immunoblotted with mouse anti-GFP and goat anti-mouse HRP. **(D-F)** Confocal

566 microscopy of 293T cells transfected with pEGFP-N1 or pFess-GFP 16 hours post-
567 transfection. Cells were mounted with ProLong Gold containing DAPI without additional
568 staining **(D)** or were stained with rabbit anti-Calreticulin **(E)** or rabbit anti-GORASP2 **(F)**
569 and Alexaflour 594 goat-anti-rabbit.
570
571 **Figure 4. Fess has separable roles in Env expression and tetherin antagonism. (A)**
572 Fess amino acid sequence (FIV C36). Approximate hydrophobic regions H1 and H2 are
573 indicated in red font, the C-region in green font, with a green arrow denoting the
574 predicted signal peptidase cleavage site (Verschoor et al., 1993). The regions deleted in
575 Δ40 and ΔH2/ΔC mutants of FIV C36 are underlined. Amino acids that are shared with
576 Rev are in teal font. **(B)** FIV-C36 Fess amino acids 1-200 were plotted for hydropathicity
577 using the Kyte and Doolittle model. H1: hydrophobic peak 1. H2: hydrophobic peak 2.
578 PCS: predicted signal peptidase cleavage site. **(C)** 293T cells lacking tetherin were
579 transfected with the indicated FIV-C36 proviral constructs, and 48 hours post-
580 transfection cell lysates were harvested and immunoblotted with cat sera reactive to FIV.
581 **(D)** CrFK cells stably expressing the FIV receptor CD134 were infected with the
582 indicated viruses which were input normalized to reverse-transcriptase content. Cells
583 were washed twice 16 hours post-infection and every other day 50 µL supernatant was
584 collected for reverse-transcriptase quantification. Spreading replication was performed
585 twice and one experiment is shown. **(E)** 293T cells with stable human or feline tetherin
586 expression were transfected and analyzed as in Figure 2A. Reverse-transcriptase
587 activity was quantified in each supernatant and the results are shown as means +/-
588 standard deviations. This was repeated three times and a representative example is
589 shown.
590
591 **Figure 5. Fess blocks virion incorporation of feline tetherin.** Control and HA-tetherin
592 expressing 293T cells were transfected with indicated FIV proviral constructs as in
593 Figure 2A. Supernatants were harvested and concentrated by ultracentrifugation over a
594 20% sucrose cushion. Concentrated virus was analyzed for reverse-transcriptase activity
595 and RT-normalized inputs were used for immunoblotting with the indicated antibodies. A
596 representative example is show for this experiment, which was repeated at least four
597 times with similar results.
598

599 **Figure S1.** Signal sequence lengths. Signal sequence lengths reported are from manual
600 assertion according to sequence analysis in the Uniprot database (UniProt Consortium,
601 2018) or were previously analyzed using the PCgene program (Pancino et al., 1994). **(A)**
602 Lentiviruses. **(B)** Human albumin, SARS-CoV-2 Spike, Ebola GP, HIV-2 Env, HIV-1 Env,
603 and FIV Env signal peptides. Hydrophobic regions are shown in red font.
604
605
606

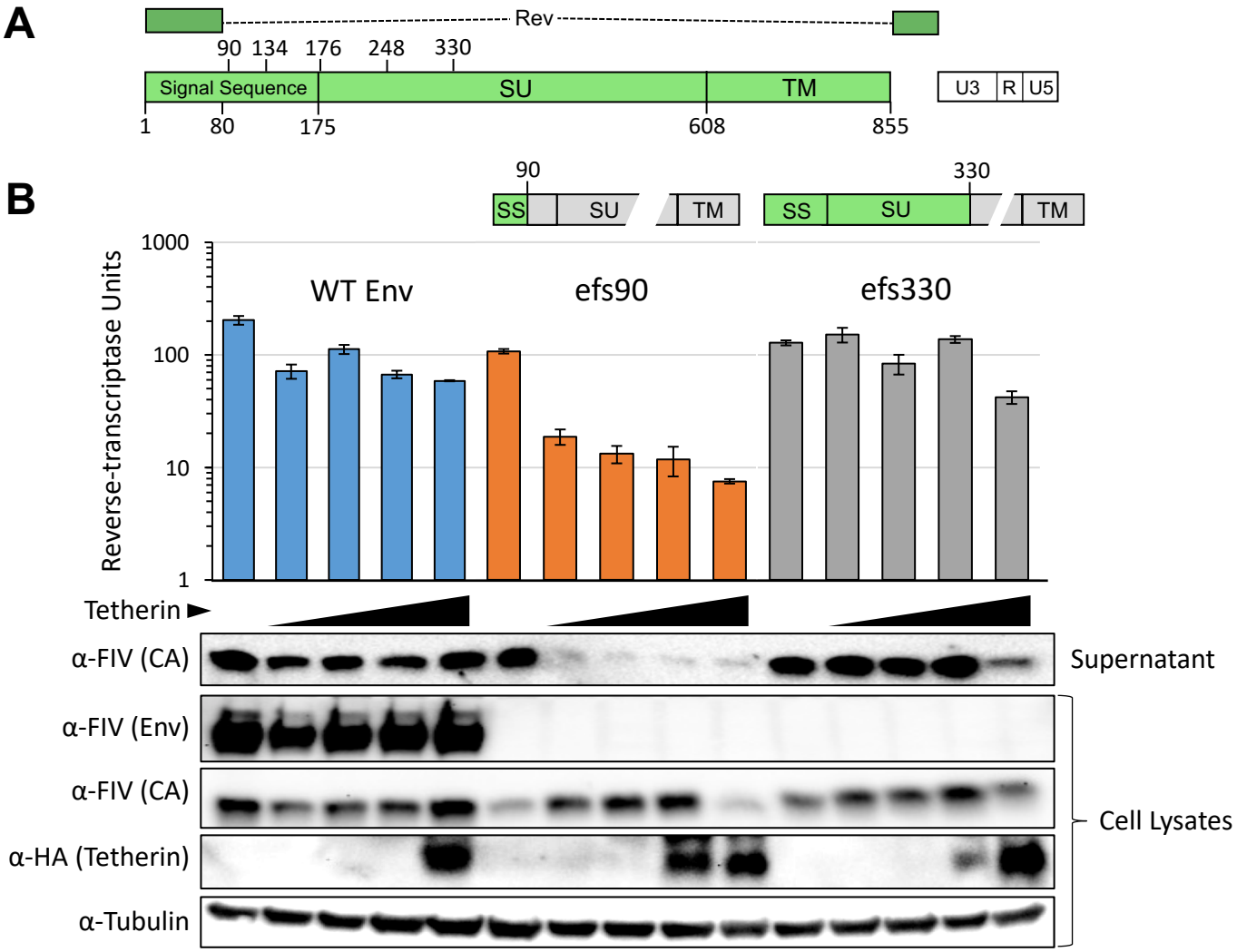

Figure 1. SU and TM are dispensable for tetherin antagonism. (A) Diagram of FIV *Env* gene. Numbering indicates amino acids from the Env initiator methionine, which is shared with Rev. **(B)** 293T cells were co-transfected with pFIVC36 proviral constructs (pCT-C36^{A+} based) encoding an intact Env (blue bars), or an Env frame-shift (efs) mutation at amino acid 90 (orange bars) or at amino acid 330 (grey bars). Diagrams indicate Env subunits intact (green) or disrupted (grey). Cell lysates and supernatant were harvested 48 hours after transfection and immunoblotted with the indicated primary antibody and a corresponding HRP-conjugated secondary antibody. Experiment was repeated four times and a representative example is shown.

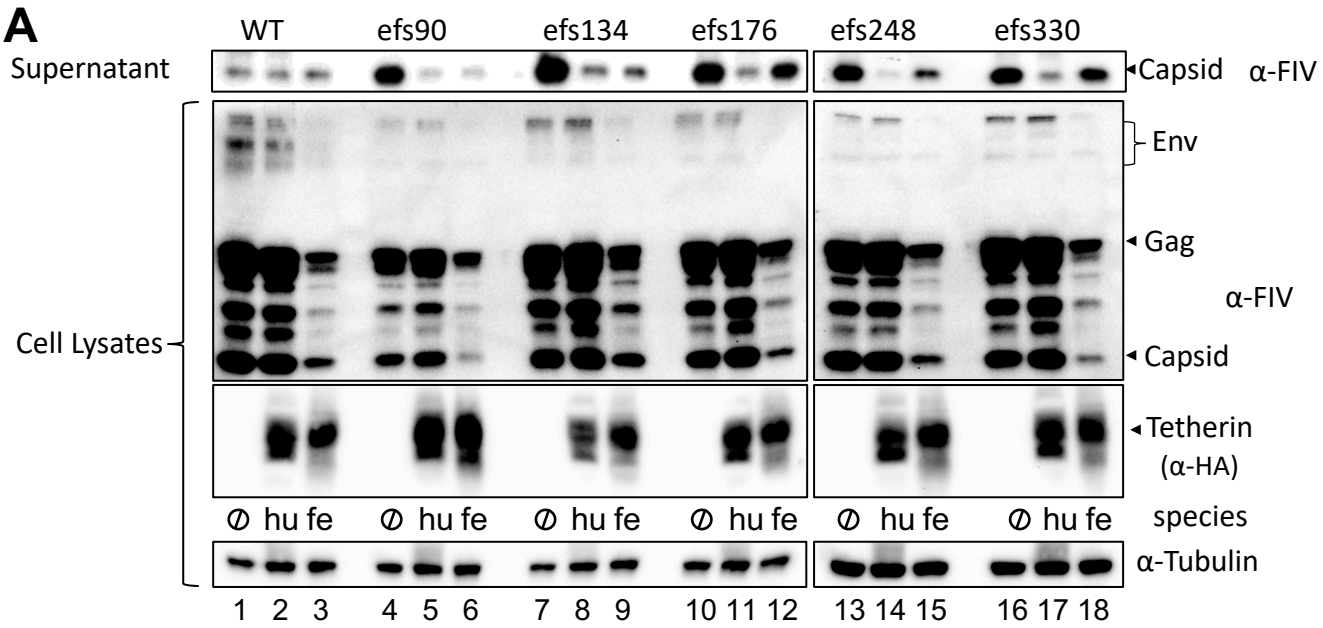

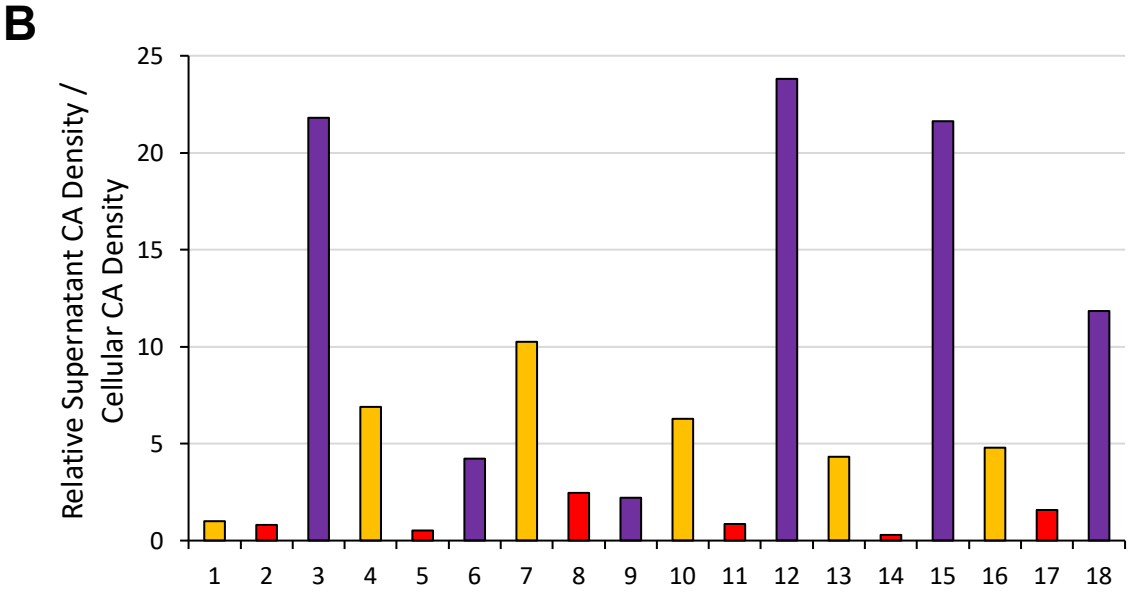

Figure 2. Effects of N-terminal deletions on feline tetherin restriction. (A) 293T cells having the indicated tetherin stably expressed under puromycin selection were transfected with the indicated pC36 proviral construct. Numbering indicates the last intact Env amino acid before early protein termination due to a frameshifting mutation. 48 hours after transfection cell lysates and supernatants were harvested and analyzed as in panel A. **(B)** Bands corresponding to FIV capsid from panel A were density quantified using ImageJ. The ratio of the supernatant to intracellular capsid band were calculated and normalized to FIVC36 from cells without tetherin. Lane numbers are the same as panel A. Experiment was repeated four times and a representative example is shown.

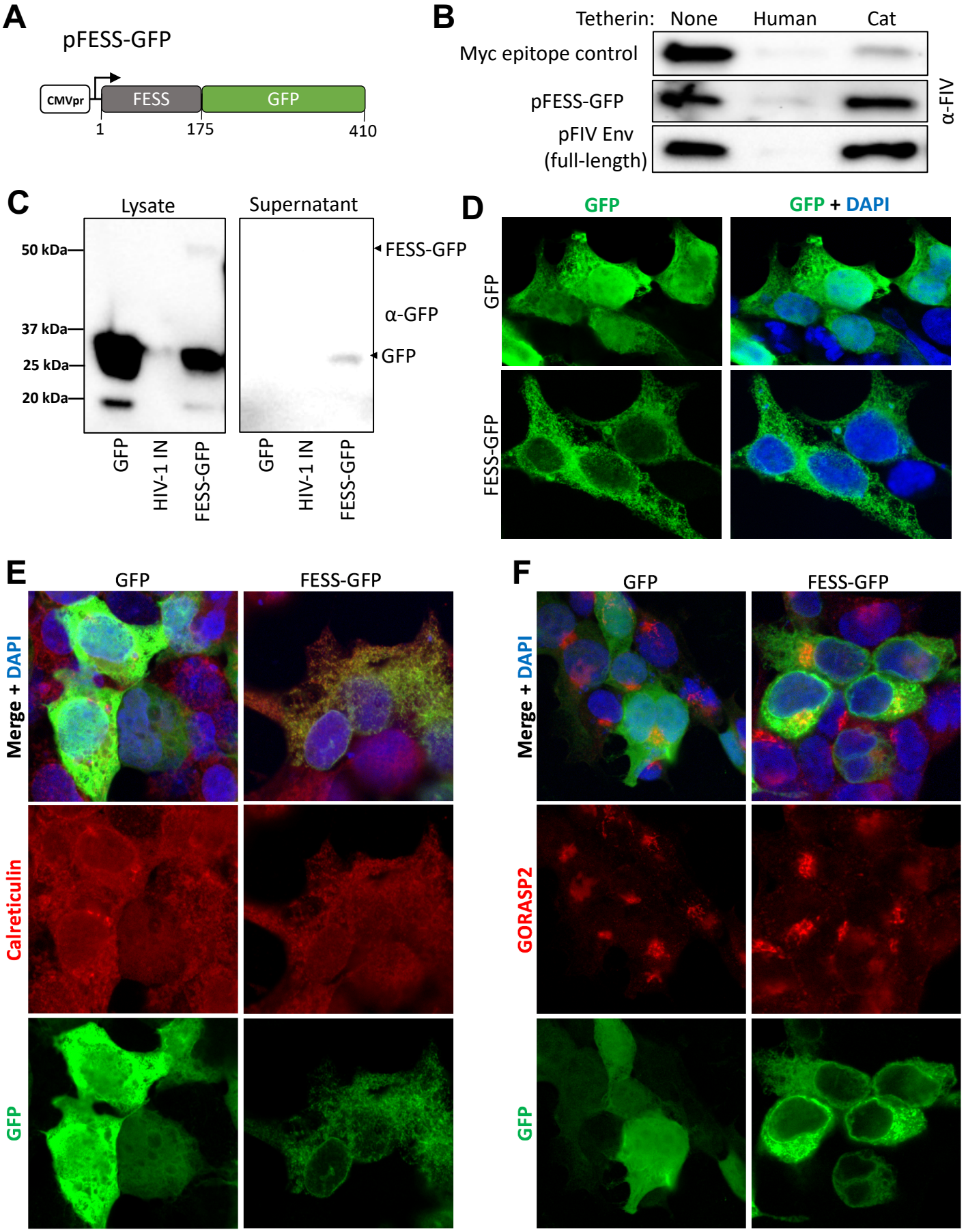

Figure 3. FESS is sufficient to counteract domestic cat Tetherin and can direct protein translocation into the secretory pathway. [Full legend in manuscript]

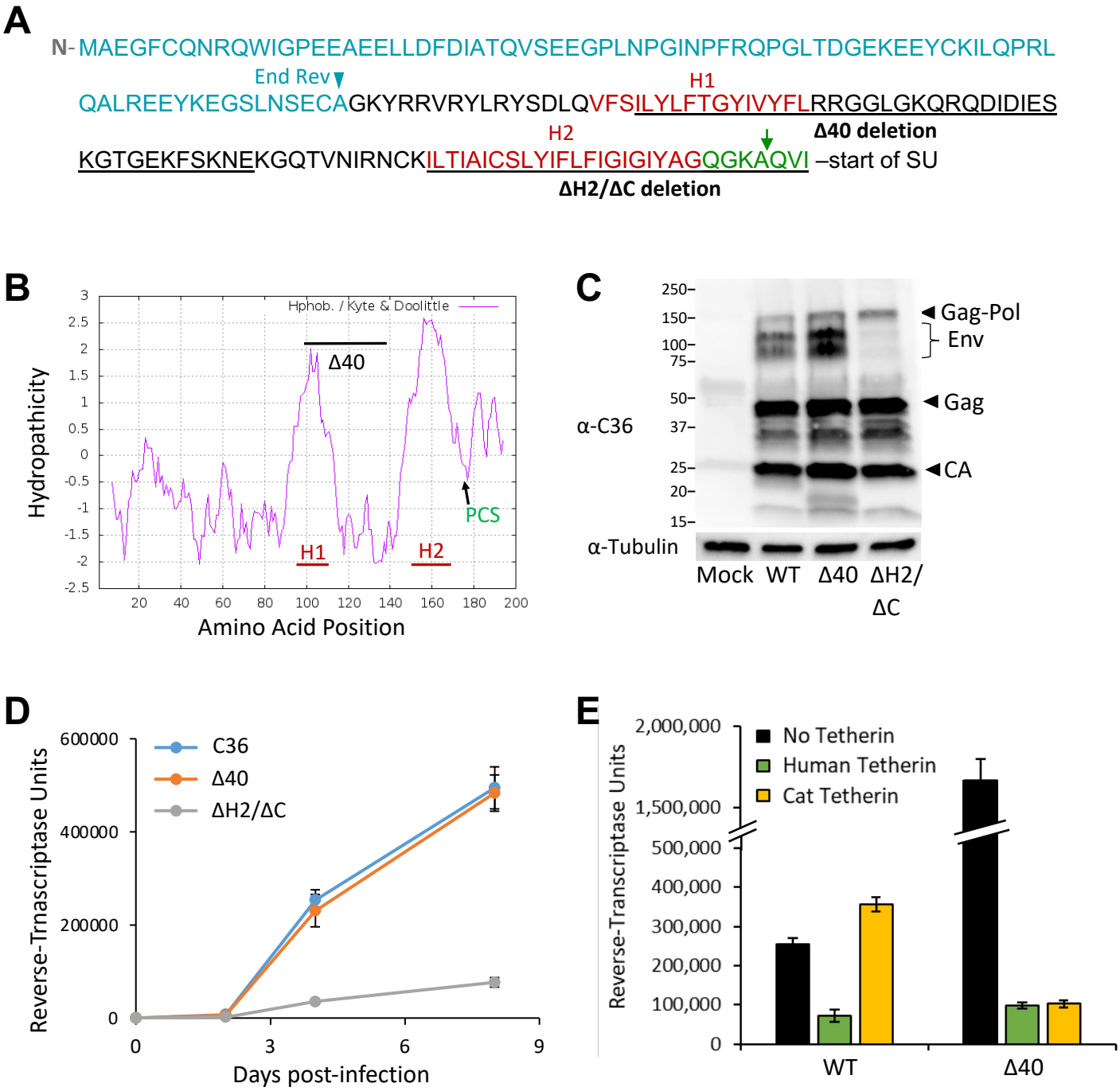

Figure 4. Fess has separable roles in Env expression and tetherin antagonism. (A) Fess amino acid sequence (FIV C36). Approximate hydrophobic regions H1 and H2 are indicated in red font, the C-region in green font, with a green arrow denoting the predicted signal peptidase cleavage site (Verschoor et al., 1993). The regions deleted in Δ40 and ΔH2/ΔC mutants of FIV C36 are underlined. Amino acids that are shared with Rev are in teal font. **(B)** FIV-C36 Fess amino acids 1-200 were plotted for hydropathicity using the Kyte and Doolittle model. H1: hydrophobic peak 1. H2: hydrophobic peak 2. PCS: predicted signal peptidase cleavage site. **(C)** 293T cells lacking tetherin were transfected with the indicated FIV-C36 proviral constructs, and 48 hours post-transfection cell lysates were harvested and immunoblotted with cat sera reactive to FIV. **(D)** CrFK cells stably expressing the FIV receptor CD134 were infected with the indicated viruses which were input normalized to reverse-transcriptase content. Cells were washed twice 16 hours post-infection and every other day 50 µL supernatant was collected for reverse-transcriptase quantification. Spreading replication was performed twice and one experiment is shown. **(E)** 293T cells with stable human or feline tetherin expression were transfected and analyzed as in Figure 2A. Reverse-transcriptase activity was quantified in each supernatant and the results are shown as means +/- standard deviations. This was repeated three times and a representative example is shown.

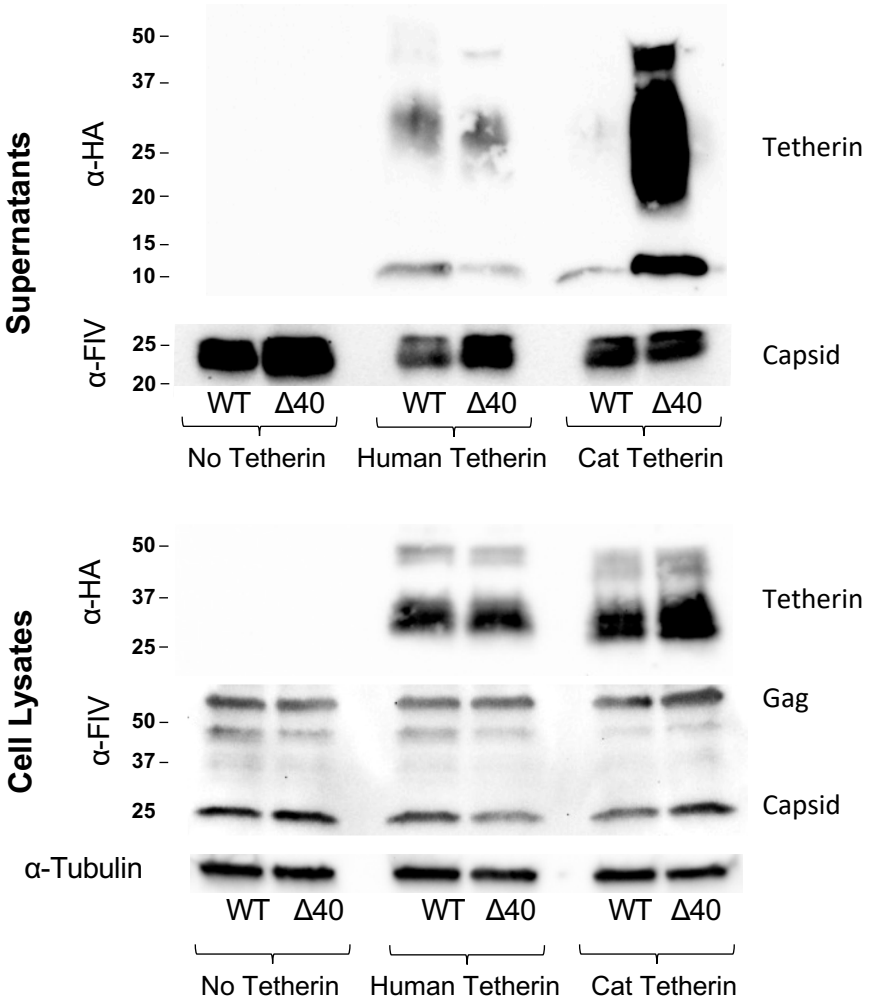

Figure 5. Fess blocks virion incorporation of feline tetherin. Control and HA-tetherin expressing 293T cells were transfected with indicated FIV proviral constructs as in Figure 2A. Supernatants were harvested and concentrated by ultracentrifugation over a 20% sucrose cushion. Concentrated virus was analyzed for reverse-transcriptase activity and RT-normalized inputs were used for immunoblotting with the indicated antibodies. A representative example is show for this experiment, which was repeated at least four times with similar results.

A

	Lentivirus	Strain	Envelope Signal Sequence Length
Non-primate	FIV	C36	175
	FIV	Petaluma	176
	Visna	KV1772	106
	EIAV		97
	CAEV	Cork	83
	BIV		83
Primate	HIV-1	NL4-3	30
	HIV-1	LAI	30
	SIVcpz	GAB1	31
	SIVsm	F235/smH4	23
	HIV-2	NIH-Z	22
	SIVcpz	TAN1	21
	SIVagm	AGM TYO-1	20
	SIVmac	Mm251	19

B

MKWVTFISLLFLFSS – **Serum Albumin**

MFVFLVLLPLVSS – **SARS-CoV-2 Spike**

MGVTGILQLPRDRFKRTSFFLWVIILFQRTFS – **Ebola Zaire GP**

MRVKEKYQHLWRWGWRWGTMLLGMLMICSA – **HIV-1 gp160**

MAYFSSRLPI ALLLIGISGFVCKQY– **HIV-2 gp140**

MAEGFCQNRQWIGPEEAEELLDFDIATQVSEEGPLNPGINPFRQPGLTDGEKEEYCKILQPRLQAL
REEYKEGSLNSECAGKYRRVRYLRYSDLQVFSILYLFTGYIVYFLRRGGLGKQRQDIDIESKGTGEK
FSKNEKGQTVNIRNCKILTIAICSLYIFLFIGIGIYAGQGKA – **FIV gp130**

Figure S1: Signal sequence lengths. Signal sequence lengths reported are from manual assertion according to sequence analysis in the Uniprot database (UniProt Consortium, 2018) or were previously analyzed using the PCgene program (Pancino et al., 1994). **(A)** Lentiviruses. **(B)** Human albumin, SARS-CoV-2 Spike, Ebola GP, HIV-2 Env, HIV-1 Env, and FIV Env signal peptides. Hydrophobic regions are shown in red font.